

Self-organized formation of step-terrace structure in SrRuO₃ thin films grown on mixed-terminated SrTiO₃ (100) substrates

Ryotaro Arakawa^{a,*}, Sachio Komori^b, Kotaro Tomita^a, Shunsei Komori^a, Masaaki A. Tanaka^c and Tomoyasu Taniyama^{a,**}

^aDepartment of Physics, Nagoya University, Nagoya, 464-8602, Aichi, Japan

^bDepartment of Physics and Electronics, Osaka Metropolitan University, Sakai, 599-8531, Osaka, Japan

^cDepartment of Physical Science and Engineering, Nagoya Institute of Technology, Nagoya, 466-8555, Aichi, Japan

ARTICLE INFO

Keywords:

SrRuO₃

Pulsed laser deposition

Step-terrace structure

Growth mode transition

Perovskite oxide thin films

ABSTRACT

Surface morphology of the substrate and bottom layers plays a critical role in the epitaxial growth of oxide thin films. Here, we report on the self-organized formation of a step-terrace structure in SrRuO₃ (SRO) thin films grown using pulsed laser deposition on mixed-terminated SrTiO₃ (100) substrates without any prior surface treatment. Atomic force microscopy observations reveal that SRO films initially grow in a three-dimensional island mode and subsequently undergo a transition to a step-flow growth mode through island coalescence as the film thickness increases, resulting in a well-defined step-terrace morphology with a step height consistent with the SRO unit-cell parameter. The average terrace width of the self-organized structure can be systematically tuned by varying the substrate temperature and the target-substrate distance, which we attribute to changes in the critical island radius that governs the nucleation behavior. To demonstrate the utility of this self-organized morphology, we show that BiFeO₃ thin films grown on SRO films with such a step-terrace structure exhibit improved surface flatness and crystalline quality compared to those grown directly on bare SrTiO₃ substrates. These findings provide a clear understanding of the mechanism of thickness-driven growth-mode transitions in perovskite oxide thin films under various growth conditions.

1. Introduction

SrRuO₃ (SRO) thin films are a widely studied perovskite material, well known for their 4*d* itinerant metallic conductivity and are commonly used as bottom electrode materials in oxide electronics [1, 2]. It is generally crucial to control the surface morphology of the bottom electrode layer to achieve high-quality epitaxial growth of subsequent layers, and SRO films are no exception [3]. In this regard, substrates with a well-defined step-terrace structure are widely employed for the growth of high-quality epitaxial films.

The surface morphology of SRO thin films, however, is known to exhibit complex growth behaviors depending on the substrate and growth conditions. For instance, SRO thin films grown on vicinal SrTiO₃ (STO) (100) substrates which possess a well-defined step-terrace structure exhibit a finger-like surface morphology in which a complete step-terrace structure fails to form at low film thicknesses [4], while in other cases the surface roughness decreases with increasing film thickness, suggesting a self-healing behavior [5]. More remarkably, SRO thin films grown on exactly-oriented STO (100) substrates entirely lacking an initial step-terrace structure have been reported to spontaneously develop a step-terrace morphology [6, 7]—a phenomenon that has not typically been observed in conventional thin-film systems, where step-terrace structures form exclusively through the diffusion of adatoms along pre-existing step edges on single-terminated substrates [8, 9, 10]. Despite these observations, the mechanism underlying this spontaneous step-terrace formation remains poorly understood.

Given that SRO is one of the most widely used bottom electrode materials in perovskite oxide heterostructures, understanding its growth mechanism and achieving flat, well-defined surface morphologies is of both fundamental and practical importance. In this study, we systematically investigate the surface morphology of SRO thin films grown on mixed-terminated STO (100) substrates without any initial step-terrace structure, with the aim of elucidating the growth mechanism responsible for the spontaneous step-terrace formation. We find that the SRO films initially grow in a three-dimensional (3D) island growth mode and subsequently transition to a step-flow growth mode through the

*Corresponding author

ORCID(s): 0000-0003-3683-5416 (T. Taniyama)

coalescence of 3D islands as the film thickness increases, resulting in a self-organized step-terrace structure with relatively well-defined step edges. Although a thickness-driven transition from 3D island growth to step-flow growth has been reported in semiconductor heteroepitaxial systems, such a systematic thickness-dependent morphological evolution has not been reported in perovskite oxide thin films.

We further show that the terrace width of the self-organized step-terrace structure is strongly influenced by the critical island radius, which can be systematically controlled by the target-substrate distance and the substrate temperature. To demonstrate the potential utility of this morphology, we show that BiFeO₃ (BFO) thin films grown on SRO films with a self-organized step-terrace structure exhibit improved surface flatness and crystalline quality compared to those grown directly on bare STO (100) substrates. These findings provide new insights into the growth mechanism of self-organized step-terrace structures in perovskite oxide thin films.

2. Experimental Methods

Epitaxial SRO thin films were grown on as-received STO (100) substrates with a miscut angle of less than 0.2° by pulsed laser deposition (PLD) using a Nd:YAG laser with a wavelength of 266 nm. The STO substrates were used without any prior surface treatment and are therefore mixed-terminated with no step-terrace structure. It is noted that droplets are commonly formed when a Nd:YAG laser is used, owing to spatially inhomogeneous ablation [11]. In this study, a 3D-shadow mask was introduced between the target and the substrate to prevent the deposition of droplets [12], successfully yielding atomically flat, highly crystalline SRO films free of droplets.

The growth conditions for SRO thin films are as follows: substrate temperature $T = 700$ and 725°C , oxygen pressure $P_{\text{O}_2} = 80$ – 120 mTorr, laser fluence $F = 6$ J/cm², repetition rate $f = 10$ Hz, target-substrate distance $d = 4$ – 4.75 cm, and deposition time $t = 30$ – 120 min, yielding a film thickness of approximately 34 nm at $t = 120$ min. To investigate the effect of the self-organized step-terrace structure on the growth of subsequent layers, BFO thin films were also grown on the SRO films under the following conditions: $T = 650^\circ\text{C}$, $P_{\text{O}_2} = 100$ mTorr, $F = 1.2$ J/cm², $f = 10$ Hz, $d = 4.5$ cm, and $t = 180$ min, yielding a film thickness of approximately 33 nm. All samples were cooled to room temperature over approximately 2 hours under $P_{\text{O}_2} = 600$ Torr immediately after growth.

The surface morphology of the films was observed by atomic force microscopy (AFM) in non-contact mode using a Park Systems NX7. The crystal structure of the films was characterized by reciprocal space mapping (RSM) using a Rigaku SmartLab X-ray diffractometer (XRD).

3. Results and Discussion

Figure 1 shows the surface morphology of the typical STO (100) substrates used in this study. The surface of the as-received STO substrate in Fig. 1(a) is flat with no step-terrace structure. We also annealed an STO substrate at 700°C for 120 min under an oxygen pressure of 100 mTorr—the same conditions as those used for SRO film growth—to examine whether a step-terrace structure can be induced by annealing at the growth temperature. The annealed STO substrate does not exhibit a clear step-terrace structure (Fig. 1(b)), which is consistent with previous reports showing that in-situ annealing of STO substrates produces large terraces with straight steps only at temperatures above 900 – 1100°C [13]. These results indicate that the self-organized formation of the step-terrace structure in SRO thin films cannot be attributed to the surface morphology of the STO substrate.

SRO films deposited on as-received STO substrates without a step-terrace structure form a well-defined step-terrace structure under growth conditions of $T = 725^\circ\text{C}$, $P_{\text{O}_2} = 100$ mTorr, and $t = 120$ min, as shown in Fig. 2. The line profile taken along the white line in Fig. 2(a) reveals a step-terrace structure with an average terrace width of approximately 220 nm and a step height of approximately 0.4 nm, comparable to the pseudocubic unit-cell parameter of SRO (~ 0.393 nm) [14]. This step-terrace morphology also forms when SRO is deposited without the 3D-shadow mask under different growth conditions (see Fig. S1); however, it is sensitive to the oxygen pressure during deposition, and a slight change in P_{O_2} leads to the considerable degradation of the step-terrace structure and the occurrence of multiple surface defects (see Fig. S2).

To investigate the growth mechanism of the self-organized step-terrace structure, we deposited SRO films for varying growth times (thickness) and observed the evolution of the surface morphology. As shown in Fig. 3, SRO films grown for 30 min exhibit a 3D island growth mode in which the surface is dominated by a high density of islands. As the growth time increases, the islands grow into elongated oval shapes roughly aligned along the [110] direction and coalesce with each other (60 min), leading to the formation of a step-terrace structure with some large residual

pits (90 min) at the junctions where adjacent islands merge. These pits are eventually filled by subsequent growth, and the step-terrace structure becomes more well defined (120 min), at which the film thickness reaches approximately 34 nm. These results demonstrate a growth-mode transition in SRO thin films on STO (100) substrates from a 3D island mode to a step-flow mode, which has been reported in semiconductor heteroepitaxial systems such as GaN on sapphire [15] and ZnSe on GaAs [16] but not in perovskite oxide thin films. This self-organized formation of a step-terrace structure is fundamentally different from the finger-like morphology previously reported for SRO films on as-received STO (100) substrates [17] in which SRO does not form complete step-terrace structures. Step-terrace structures are typically formed either by the coalescence of two-dimensional (2D) islands on a terrace referred to as layer-by-layer growth [18] or by the diffusion of adatoms to step edges, referred to as step-flow growth [19]. In either case, a single-terminated substrate with a well-defined step-terrace structure is required for the overlying film to develop a step-terrace morphology.

It should also be noted that the average terrace width L_{ave} of the self-organized step-terrace structure is larger for SRO films grown at 725°C (Fig. 2(a)) than for those grown at 700°C (Fig. 3(d)), approximately 220 nm and 120 nm, respectively. This difference can be attributed to the critical island radius R_c , which defines the minimum island size that can remain stable against the re-evaporation of adatoms [20] and is governed by thermal conditions such as the substrate temperature. When R_c is smaller than the island separation, new islands tend to nucleate on top of existing 2D islands, giving rise to 3D island structures [21]. For SRO films grown at 725°C (Fig. 4(a)), the elevated substrate temperature suppresses the nucleation of small, unstable islands, resulting in a larger R_c , larger islands, and consequently a larger L_{ave} after coalescence. In contrast, a lower substrate temperature of 700°C (Fig. 4(b)) favors a smaller R_c , leading to finer islands and a smaller L_{ave} .

It has been theoretically shown for multilayer growth [22], in which 3D islands composed of bottom-2D island with a radius ρ_1 and top-2D island with a radius ρ_2 grow simultaneously ($\rho_1 > \rho_2$), that $\rho_1^2 - \rho_2^2$ is proportional to $1/N_s$, where N_s denotes the saturation island density, which is inversely related to R_c . In this configuration, the quantity $\rho_1 - \rho_2$ represents the lateral distance between the edges of the upper and lower islands, corresponding to the step-terrace width that self-organizes in this study. A higher substrate temperature increases R_c , which in turn decreases N_s and leads to an increase in $\rho_1 - \rho_2$, consistent with the larger L_{ave} observed at 725°C.

This growth picture is further supported by the dependence of L_{ave} on the target-substrate distance d , as shown in Fig. 5. SRO films grown with $d = 4.0$ cm exhibit a very small L_{ave} of approximately 73 nm (Fig. 5(a)), accompanied by some large square-shaped pits, whereas those grown with $d = 4.75$ cm exhibit flat terraces with a larger L_{ave} of approximately 110 nm (Fig. 5(d)). Notably, L_{ave} increases linearly with increasing d , as shown in Fig. 5(e). This difference in L_{ave} can be attributed to the kinetic energy of the incident atoms, which is governed by d . At smaller d (Fig. 6(a)), the incident atoms possess higher kinetic energy, leading to local surface damage such as pit formation through energetic collisions with the substrate. These pits serve as preferential nucleation sites, resulting in a higher nucleation density, smaller islands, and a reduced R_c , ultimately yielding a smaller L_{ave} . At larger d (Fig. 6(b)), the lower kinetic energy suppresses pit formation, allowing islands to grow more stably and increasing both R_c and L_{ave} . This interpretation agrees with kinetic Monte Carlo simulations of PLD film growth, which show that energetic collisions can split unstable small islands into single adatoms, thereby increasing nucleation density and decreasing the average island size [23].

We also investigated the effect of the self-organized step-terrace structure in SRO thin films on the growth of subsequent layers by depositing BFO thin films with a thickness of approximately 33 nm. BFO thin films grown directly on as-received STO substrates without a step-terrace structure undergo Volmer–Weber growth, yielding a rough surface dominated by 3D islands with a root-mean-square roughness of approximately 5.2 nm (Fig. 7(a)). Since the surface morphology of BFO films is highly sensitive to the surface structure of the underlying substrate [24, 25], BFO films grown on mixed-terminated STO (100) substrates typically exhibit an inhomogeneous surface morphology and are prone to the formation of impurity phases such as Bi₂O₃ or Fe₂O₃ [26].

In contrast, BFO thin films grown on SRO films with a self-organized step-terrace structure—specifically those grown under the conditions of Fig. 5(b)—exhibit a significantly smaller root-mean-square roughness of approximately 0.56 nm (Fig. 7(b)). Although the growth mode is not a perfect step-flow but rather step-bunching, in which multiple steps coalesce, further optimization of the growth conditions could enable true step-flow growth of BFO films. The crystal structure of these BFO films was also evaluated by RSM around the (103) STO Bragg peaks (Figs. 7(c) and (d)), with all reciprocal-space coordinates normalized to those of STO ($= 1/0.3905 \text{ nm}^{-1}$) [27]. In both samples, the BFO films exhibit a single RSM peak, confirming *c*-axis-aligned growth without any impurity phases. The BFO peak is sharper in the BFO/SRO/STO sample than in the BFO/STO sample, indicating improved crystalline quality owing

to the self-organized step-terrace structure of the SRO underlayer. These results demonstrate that the self-organized step-terrace morphology effectively reduces surface roughness and enhances the crystalline quality of subsequently deposited films. The ferroelectric response of BFO/SRO/STO was further evaluated by piezoelectric force microscopy, confirming a clear ferroelectric domain structure (see Fig. S3).

4. Conclusion

In conclusion, we have elucidated the growth mechanism responsible for the self-organized formation of step-terrace structures in SrRuO₃ films grown on mixed-terminated STO (100) substrates without any initial step-terrace structure. Systematic thickness-dependent observations reveal a clear growth-mode transition from 3D island growth to step-flow growth as the film thickness increases, driven by the coalescence of 3D islands. The terrace width of the resulting self-organized step-terrace structure can be tuned by adjusting the substrate temperature and the target-substrate distance, which we attribute to the corresponding changes in the critical island radius governing the nucleation behavior. These findings provide a clear understanding of the mechanism of thickness-driven growth-mode transitions in perovskite oxide thin films under various growth conditions. As a further demonstration, ferroelectric BiFeO₃ films grown on SRO films with this self-organized step-terrace structure exhibit improved surface morphology and crystallinity compared to those grown directly on bare STO substrates, suggesting that this morphology may also serve as a useful template for subsequent epitaxial growth.

Appendix A: Supplementary data

The data that support the findings of this study are available from the corresponding author upon reasonable request.

CRediT authorship contribution statement

Ryotaro Arakawa: Conceptualization, Methodology, Writing – original draft, Writing – review & editing, Data curation, Formal analysis, Visualization, Validation, Software, Investigation. **Sachio Komori:** Supervision, Writing – review & editing. **Kotaro Tomita:** Investigation, Methodology. **Shunsei Komori:** Investigation, Validation. **Masaaki A. Tanaka:** Methodology. **Tomoyasu Taniyama:** Supervision, Resources, Funding acquisition, Project administration, Writing – review & editing.

Declaration of competing interest

The authors declare no competing financial interests.

Declaration of generative AI use in scientific writing

The authors used generative AI tools (Microsoft Copilot and Claude) only for language refinement. All scientific content, data interpretation, and conclusions were generated by the authors.

Acknowledgments

This work was supported in part by JSPS KAKENHI Grant Nos. JP23KK0086, JP24H00380, JP24K21732, JSPS International Joint Research Program (JRP-LEAD with UKRI) No. JPJSJRP20241705, JST FOREST Grant No. JPMJFR212V.

Data availability

The data that support the findings of this study are available from the corresponding author upon reasonable request.

References

- [1] Y. J. Chang, C. H. Kim, S.-H. Phark, Y. Kim, J. Yu, T. Noh, Fundamental thickness limit of itinerant ferromagnetic SrRuO₃ thin films, *Phys. Rev. Lett.* 103 (2009) 057201.

- [2] M. Cuoco, A. Di Bernardo, Materials challenges for SrRuO₃: From conventional to quantum electronics, *APL Mater.* 10 (2022) 090902.
- [3] H. Wang, Z. Wang, Z. Ali, E. Wang, M. Saghayezhian, J. Guo, Y. Zhu, J. Tao, J. Zhang, Surface termination effect of SrTiO₃ substrate on ultrathin SrRuO₃, *Phys. Rev. Mater.* 8 (2024) 013605.
- [4] F. Sánchez, G. Herranz, I. Infante, J. Fontcuberta, M. García-Cuenca, C. Ferrater, M. Varela, Critical effects of substrate terraces and steps morphology on the growth mode of epitaxial SrRuO₃ films, *Appl. Phys. Lett.* 85 (2004) 1981–1983.
- [5] D. Rubi, A. Vlooswijk, B. Noheda, Growth of flat SrRuO₃ (111) thin films suitable as bottom electrodes in heterostructures, *Thin Solid Films* 517 (2009) 1904–1907.
- [6] T. Zhu, L. Lu, X. Zhao, Z. Ji, J. Ma, Epitaxial growth and ferroelectric properties of Pb(Zr_{0.52}Ti_{0.48})O₃/SrRuO₃ heterostructures on exact SrTiO₃ (001) substrates, *J. Cryst. Growth* 291 (2006) 385–389.
- [7] Z.-Z. Jiang, Z. Guan, N. Yang, P.-H. Xiang, R.-J. Qi, R. Huang, P.-X. Yang, N. Zhong, C.-G. Duan, Epitaxial growth of BiFeO₃ films on SrRuO₃/SrTiO₃, *Mater. Charact.* 131 (2017) 217–223.
- [8] W. Hong, H. N. Lee, M. Yoon, H. M. Christen, D. H. Lowndes, Z. Suo, Z. Zhang, Persistent step-flow growth of strained films on vicinal substrates, *Phys. Rev. Lett.* 95 (2005) 095501.
- [9] H. N. Lee, H. M. Christen, M. F. Chisholm, C. M. Rouleau, D. H. Lowndes, Thermal stability of epitaxial SrRuO₃ films as a function of oxygen pressure, *Appl. Phys. Lett.* 84 (2004) 4107–4109.
- [10] H. Schraknepper, C. Bäumer, R. Dittmann, R. A. De Souza, Complex behaviour of vacancy point-defects in SrRuO₃ thin films, *Phys. Chem. Chem. Phys.* 17 (2015) 1060–1069.
- [11] S. Chaluvadi, D. Mondal, C. Bigi, D. Knez, P. Rajak, R. Ciancio, J. Fujii, G. Panaccione, I. Vobornik, G. Rossi, et al., Pulsed laser deposition of oxide and metallic thin films by means of Nd:YAG laser source operating at its 1st harmonics: recent approaches and advances, *J. Phys.: Mater.* 4 (2021) 032001.
- [12] M. Tachiki, T. Kobayashi, An improved laser ablation method using a shadow mask (eclipse method), *Electr. Eng. Jpn.* 130 (2000) 88–94.
- [13] M. Jäger, A. Teker, J. Mannhart, W. Braun, Independence of surface morphology and reconstruction during the thermal preparation of perovskite oxide surfaces, *Appl. Phys. Lett.* 112 (2018) 111601.
- [14] G. Koster, L. Klein, W. Siemons, G. Rijnders, J. S. Dodge, C.-B. Eom, D. H. Blank, M. R. Beasley, Structure, physical properties, and applications of SrRuO₃ thin films, *Rev. Mod. Phys.* 84 (2012) 253–298.
- [15] K. Takemura, T. Fukui, Y. Matsuda, M. Funato, Y. Kawakami, Metal-organic vapor phase epitaxy of high-quality GaN on Al-pretreated sapphire substrates without using low-temperature buffer layers, *Phys. Status Solidi B* 261 (2024) 2400043.
- [16] X. B. Zhang, K. L. Ha, S. K. Hark, Thickness dependent surface morphologies and luminescent properties of ZnSe epilayers grown on (001) GaAs by metalorganic chemical vapor phase deposition, *J. Cryst. Growth* 223 (2001) 528–534.
- [17] F. Sánchez, G. Herranz, I. Infante, C. Ferrater, M. Garcia-Cuenca, M. Varela, J. Fontcuberta, Growth modes and self-organization in the epitaxy of ferromagnetic SrRuO₃ on SrTiO₃ (001), *Prog. Solid State Chem.* 34 (2006) 213–221.
- [18] Y. J. Chang, S.-h. Phark, Direct nanoscale analysis of temperature-resolved growth behaviors of ultrathin perovskites on SrTiO₃, *ACS Nano* 10 (2016) 5383–5390.
- [19] T. F. Kuech (Ed.), *Handbook of Crystal Growth: Thin Films and Epitaxy: Basic Techniques*, volume III, Part A, Elsevier, second edition, 2015.
- [20] J. G. Amar, F. Family, Critical cluster size: Island morphology and size distribution in submonolayer epitaxial growth, *Phys. Rev. Lett.* 74 (1995) 2066.
- [21] J. Tersoff, A. D. Van Der Gon, R. Tromp, Critical island size for layer-by-layer growth, *Phys. Rev. Lett.* 72 (1994) 266.
- [22] I. V. Markov, *Crystal Growth for Beginners: Fundamentals of Nucleation, Crystal Growth and Epitaxy*, World Scientific Publishing Co. Pte. Ltd., Hackensack, New Jersey and Singapore, 3rd edition, 2016.
- [23] D. Zhang, L. Guan, Z. Li, G. Pan, X. Tan, L. Li, Simulation of island aggregation influenced by substrate temperature, incidence kinetic energy and intensity in pulsed laser deposition, *Appl. Surf. Sci.* 253 (2006) 874–880.
- [24] H. W. Jang, D. Ortiz, S.-H. Baek, C. M. Folkman, R. R. Das, P. Shafer, Y. Chen, C. T. Nelson, X. Pan, R. Ramesh, et al., Domain engineering for enhanced ferroelectric properties of epitaxial (001) BiFeO₃ thin films, *Adv. Mater.* 21 (2009) 817–823.
- [25] T. Zhang, J. Li, M. Zhao, L. Wu, Q. Chen, J. Ma, J. Yi, Manipulation of BiFeO₃ nanostructure by substrate terrace morphology, *Appl. Surf. Sci.* 648 (2024) 159088.
- [26] H. Toupet, F. Le Marrec, J. Holc, M. Kosec, P. Vilarhino, M. Karkut, Growth and thermal stability of epitaxial BiFeO₃ thin films, *J. Magn. Magn. Mater.* 321 (2009) 1702–1705.
- [27] Y.-H. Chu, M. P. Cruz, C.-H. Yang, L. W. Martin, P.-L. Yang, J.-X. Zhang, K. Lee, P. Yu, L. Q. Chen, R. Ramesh, Domain control in multiferroic BiFeO₃ through substrate vicinality, *Adv. Mater.* 19 (2007) 2662.

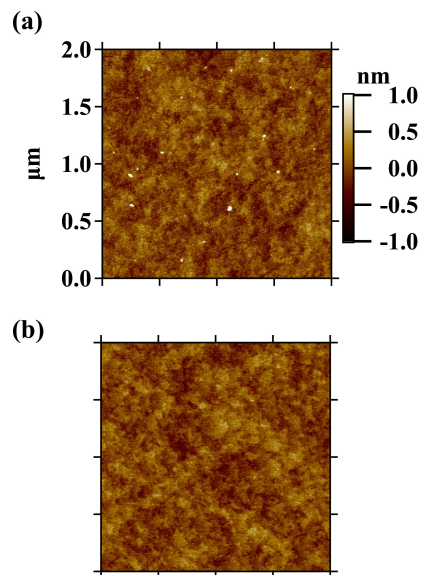


Figure 1: Surface morphology of (a) as-received and (b) PLD-annealed ($T = 700^{\circ}\text{C}$, $P_{\text{O}_2} = 100$ mTorr, $t = 120$ min) STO substrates.

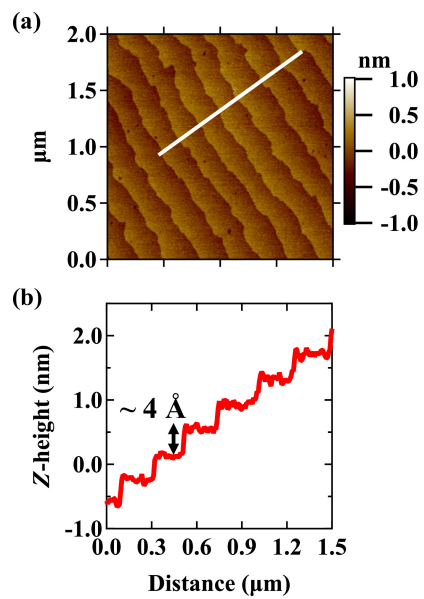


Figure 2: Surface morphology of 34 nm-thick-SRO thin films on a bare STO substrate ($T = 725^{\circ}\text{C}$, $P_{\text{O}_2} = 100$ mTorr, $t = 120$ min). (a) AFM image and (b) line profile along the white solid line after plane-fit leveling.

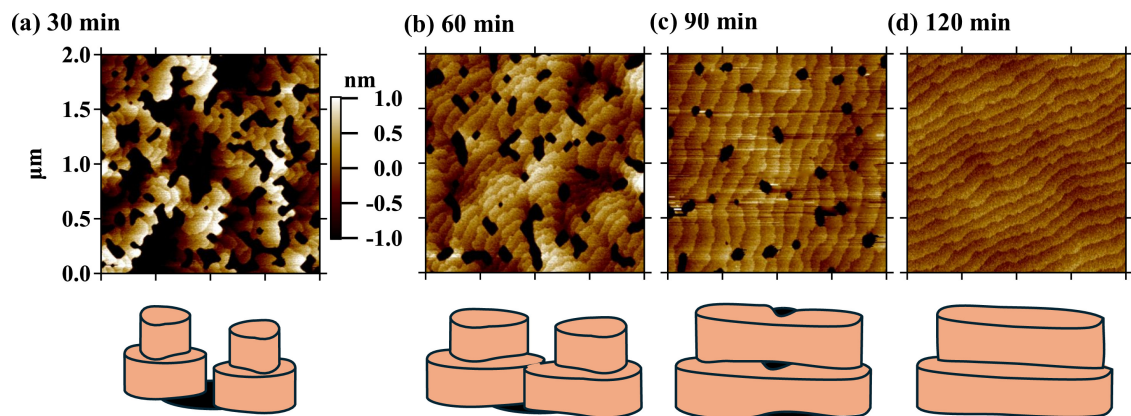


Figure 3: Surface morphology of SRO/STO ($T = 700^{\circ}\text{C}$, $P_{\text{O}_2} = 100$ mTorr, $d = 4.5$ cm) and growth schematics of the self-organized step-terrace structure at different growth times: (a) $t = 30$ min, (b) 60 min, (c) 90 min, and (d) 120 min. The SRO film grown for 120 min has a thickness of approximately 34 nm. All AFM images are acquired over a $2\ \mu\text{m} \times 2\ \mu\text{m}$ scan area.

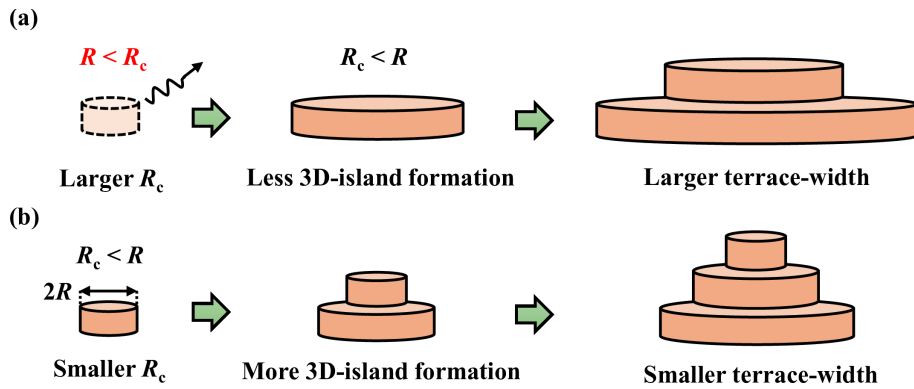


Figure 4: Schematic illustration of island growth mechanisms at the SRO/STO interface at (a) 725°C and (b) 700°C.

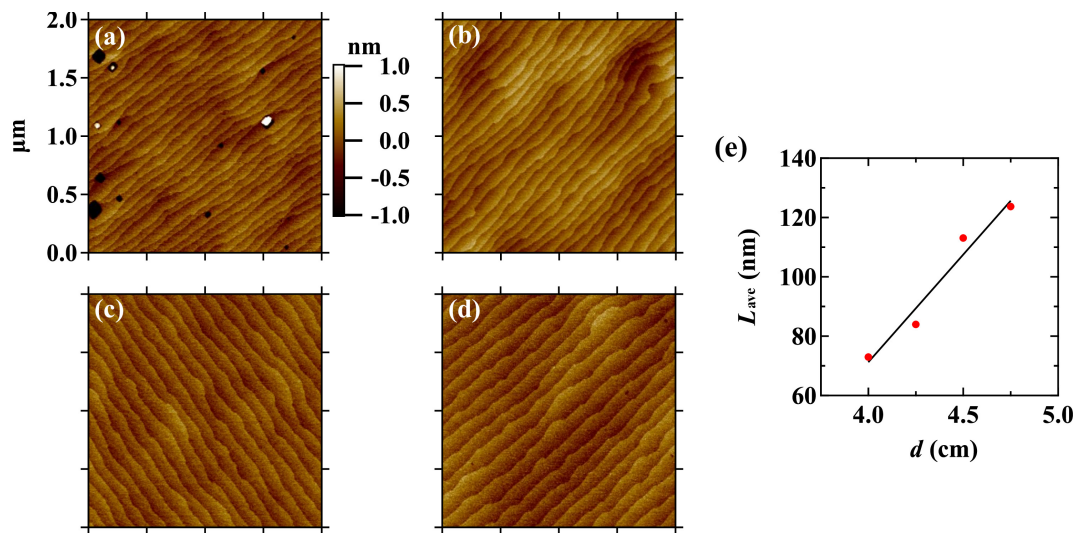


Figure 5: Surface morphology of SRO/STO ($T = 700^\circ\text{C}$, $P_{\text{O}_2} = 100$ mTorr, $t = 120$ min, thickness ≈ 34 nm) for different target-substrate distances: (a) $d = 4.0$ cm, (b) 4.25 cm, (c) 4.5 cm, and (d) 4.75 cm. (e) Average terrace width L_{ave} as a function of d . All AFM images are acquired over a $2 \mu\text{m} \times 2 \mu\text{m}$ scan area.

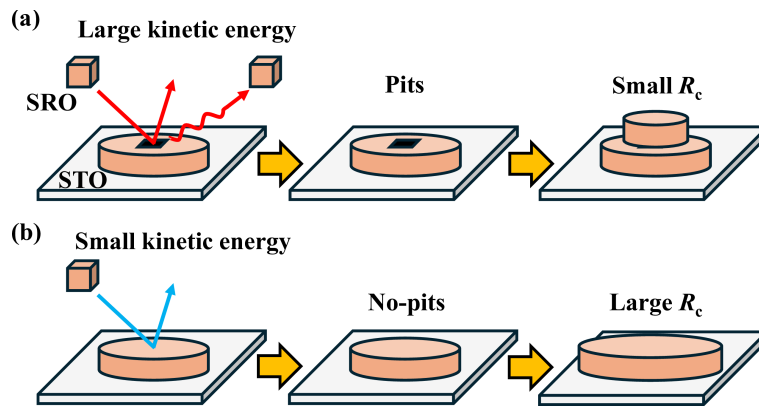


Figure 6: Schematic illustration of island growth mechanisms of SRO films with (a) smaller and (b) larger d .

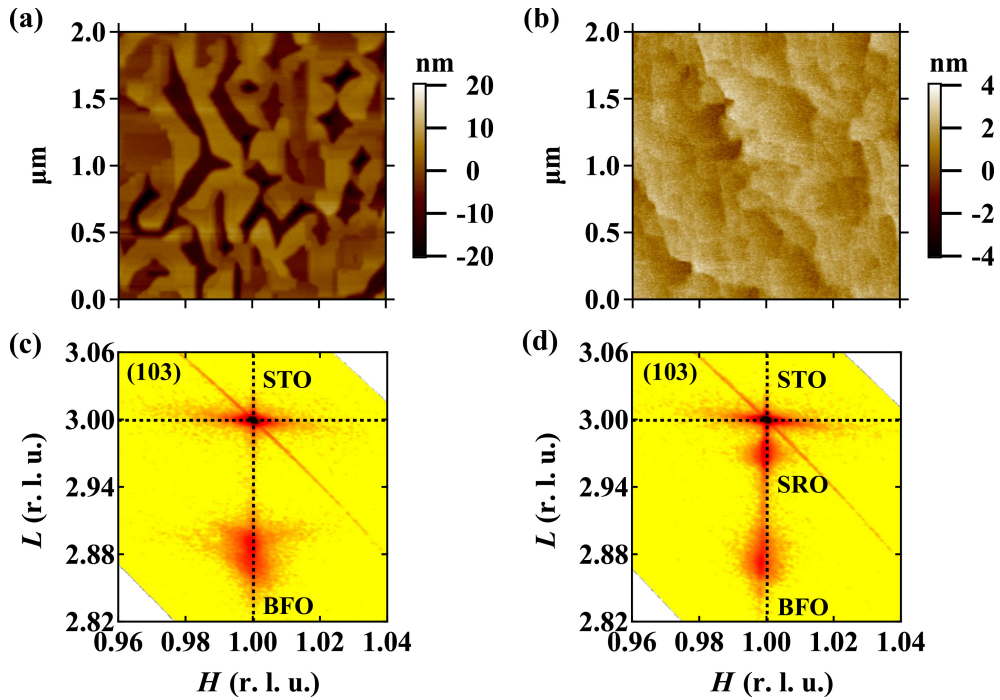


Figure 7: Surface morphology of 33 nm-thick-BFO thin films grown under identical conditions on (a) the as-received STO substrate and (b) the SRO/STO sample exhibiting a self-organized step-terrace structure. The corresponding root-mean-square roughness values are approximately 5.2 nm and 0.56 nm, respectively. (c) and (d) show the RSM patterns for the respective samples.

Supplementary Materials

Growth of SRO/STO without using shadow-mask

We deposited SRO on a mixed-terminated STO (100) substrate without using a shadow mask in a separate PLD chamber under different growth conditions: $T = 650^{\circ}\text{C}$, $P_{\text{O}_2} = 400$ mTorr, $F = 4.2$ J/cm², $f = 10$ Hz, $d = 4$ cm, cooling under 600 Torr, $t = 15$ min (thickness = 12.7 nm). SRO was found to spontaneously form a step-terrace morphology even without the shadow mask, although droplets are also present (Fig. S1). This confirms that the self-organized step-terrace formation is an intrinsic feature of SRO growth on mixed-terminated STO substrates, independent of the shadow-mask deposition. It is also noteworthy that the step-flow growth mode is established at a smaller film thickness than that observed in the shadow-mask experiments. Moreover, the average terrace width of approximately 185 nm is remarkably large compared to the values of 70–130 nm observed in the shadow-mask experiments (Fig. 5(e)), despite the lower substrate temperature of 650°C relative to the 700°C used in those experiments. These observations suggest that the relatively higher adatom diffusivity resulting from the absence of the shadow mask increases the critical island radius, promoting faster island coalescence and an earlier onset of step-flow growth at a smaller film thickness, as well as wider terraces after coalescence.

Influence of oxygen pressure on the SRO surface morphology

The surface morphology of SRO thin films is strongly dependent on the oxygen pressure during growth (Fig. S2). A self-organized step-terrace structure forms only at the optimal oxygen pressure of 100 mTorr. At oxygen pressures of 80 or 120 mTorr, the surface becomes unstable and exhibits large pits, indicating a narrow optimal window for the step-flow growth mode. These results highlight the importance of precisely controlling the oxygen pressure.

Ferroelectric properties of BFO/SRO/STO

The ferroelectric properties of BFO thin films deposited on SRO films with a self-organized structure were evaluated by piezoelectric force microscopy (PFM) in contact-resonance mode at room temperature using a Park Systems NX7. Prior to the PFM measurements, part of the BFO thin film was etched using KPZ-04 solution to expose the SRO layer as a bottom electrode. PFM phase, amplitude, and topographic (z-height) images were acquired as shown in Fig. S3. Figures S3(a) and (b) show clear contrast in the lateral PFM phase and amplitude, whereas no contrast was observed in the vertical PFM phase signal (not shown). Since 71° domains share the same out-of-plane polarization component, the vertical PFM signal is uniform across the film and thus shows no contrast between domains. The clear lateral PFM contrast therefore confirms the presence of a 71° ferroelectric domain structure.

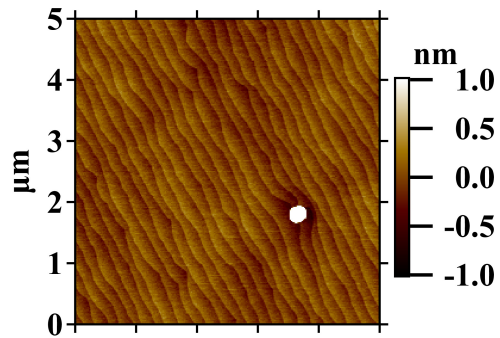


Figure S1: Surface morphology of 12.7 nm-thick-SRO deposited on mixed-terminated STO (100) without using the 3D-shadow mask.

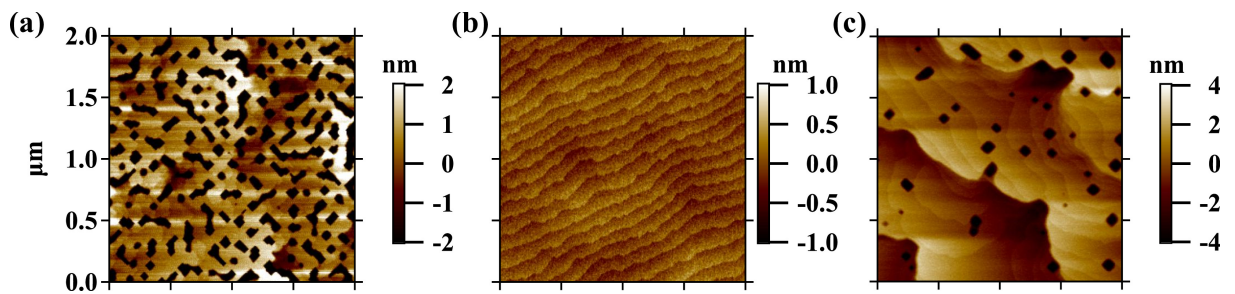


Figure S2: Surface morphology of SRO/STO grown under oxygen pressures of (a) 80 mTorr, (b) 100 mTorr, and (c) 120 mTorr. All AFM images were acquired over a $2 \mu\text{m} \times 2 \mu\text{m}$ scan area.

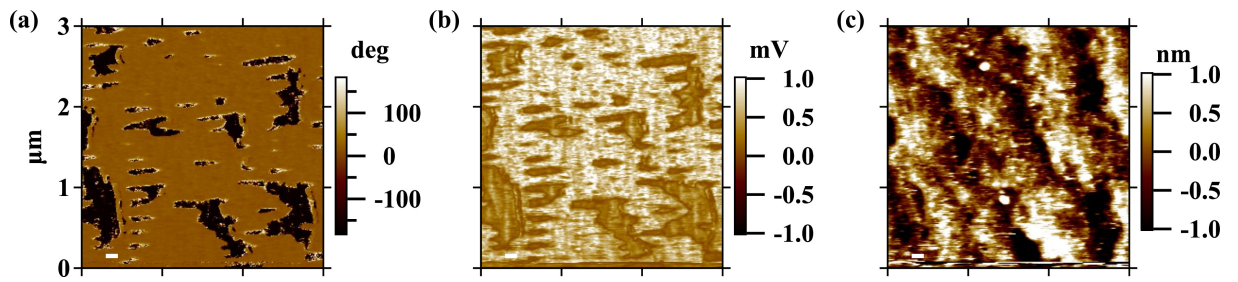


Figure S3: Lateral PFM images of BFO/SRO/STO: (a) phase, (b) amplitude, and (c) z-height. All images were obtained over a $3\ \mu\text{m} \times 3\ \mu\text{m}$ scan area.